Angewandte Chemie
Eine Zeitschrift der Gesellschaft Deutscher Chemiker

Supporting Information

Expanding Reaction Horizons: Evidence of the 5-Deazaflavin Radical Through Photochemically Induced Dynamic Nuclear Polarization

*J. Wörner, S. Panter, B. Illarionov, A. Bacher, M. Fischer, S. Weber**

Supporting Information

Contents

1 Materials and Methods

1.1 Sample Preparation

L-Tryptophan and D_2O (99.9 %) were purchased from Sigma-Aldrich. NaOD (40 % w/w, 99.5 % D) and DCl (22 % w/w, 99.5 % D) were purchased from Cambridge Isotope Laboratories. L-Tyrosine was purchased from Carl Roth GmbH + Co. KG. These chemicals were used without further purification. 5-DeazaFMN was synthesized following a procedure described by O'Brien *et al.* [1] and purified by high-performance liquid chromatography (HPLC) (LiChrospher RP-18 column, 150 mm × 20 mm) by using a linear 12−30 % gradient of methanol in water (flow rate: 10 mL/min, retention time: 18 min).

For the preparation of NMR samples, 5-deazaFMN was dissolved in D_2O at a concentration of 0.8 mM. CIDNP samples were prepared to contain 0.20 mM of 5-deazaFMN and 5 mM of L-tryptophan or 1.3 mM of L-tyrosine. The samples were subsequently adjusted to the respective pH value by addition of small amounts of NaOD and DCl.

1.2 NMR and Photo-CIDNP Spectroscopy

For the NMR experiments a Bruker Avance III HD 14.1 T NMR spectrometer (Bruker BioSpin GmbH, Rheinstetten, Germany) and a triple-resonance TXI probe optimized for proton experiments were used. All experiments were performed at 293 K. For the acquisition of thermally polarized ^{1}H spectra a standard pulse sequence was employed. Photo-CIDNP experiments were performed as previously described [2]. The samples were illuminated by insertion of an optical fiber (diameter: 1 mm, Thorlabs, Dachau, Germany) into the NMR tube via a coaxial insert (Wilmad WGS-5BL). For light excitation a system comprising a nanosecond-pulsed Nd:YAG laser (Surelite I, Continuum, Santa Clara, CA, USA) and a broadband OPO (Continuum OPO PLUS) was used. The excitation wavelength was set to 420 nm. For photo-CIDNP experiments a pulse sequence with a presaturation pulse train and destruction of thermal polarization prior to light excitation according to Goez *et al.* [3] as well as a destructive phase cycle was used. To obtain relative CIDNP intensities the CIDNP signals were fitted with the function achieving the highest correlation. A Lorentzian function was used for all signals with the exceptions of H9 at pH 6.6, H6 and H7α at pH 8.7 and H9 at pH 10.1 for which a Gaussian function was used.

1.3 Density Functional Theory Calculations

DFT calculations were performed with the ORCA program package (ORCA version 5.0) [4, 5]. Geometry optimizations were carried out by using the B3LYP functional [6] and the TZVP basis set [7]. Subsequent calculation of hyperfine coupling constants and **g**-tensors were performed with the B3LYP functional and the IGLO-II basis set [8]. Additionally, the CPCM model [9] was used to simulate water solvation.

2 Assignments of ^{1}H Resonances in 5-DeazaFMN

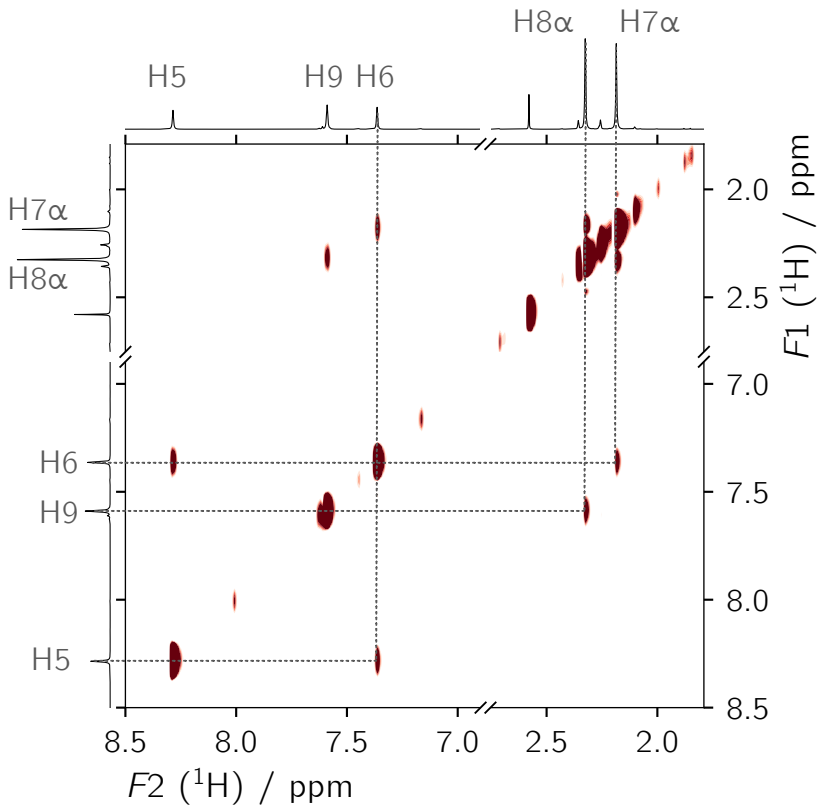

Figure S1 Two-dimensional NOESY spectrum of 5-deazaFMN in D_2O. For acquisition a gradient-selected, phase-sensitive standard pulse sequence with solvent suppression by excitation sculpting was used [10–12] and a mixing time of 900 ms was chosen. Zero-filling was applied as well as line-broadening of 1.00 Hz and 0.30 Hz in $F2$ and $F1$ respectively prior to Fourrier transformation. The spectrum was phase-corrected in $F2$. Cross-peaks between H7α and H6, H6 and H5 as well as H8α and H9 are marked.

3 pH Dependence of ^{1}H Resonances in 5-DeazaFMN

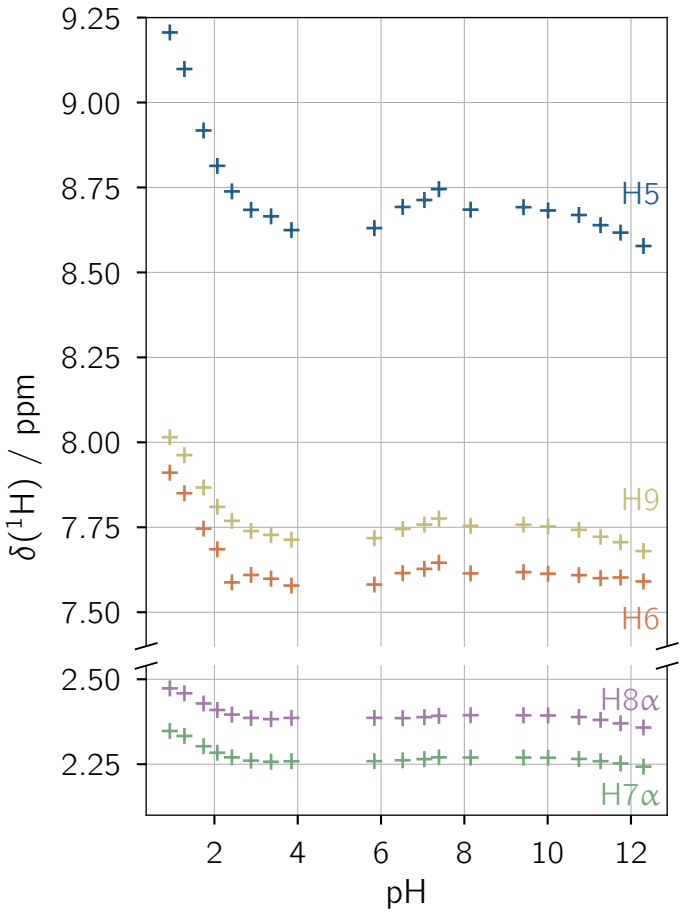

Figure S2 pH dependence from pH 0.9 to 12.3 of ^{1}H chemical shifts for 5-DeazaFMN. The values for nuclei of the aromatic 5-deazaFMN moiety are depicted. The chemical shifts were calibrated using the signal of residual HDO at 4.7 ppm.

4 Density Functional Theory Calculations of 5-DeazaFMN Radicals

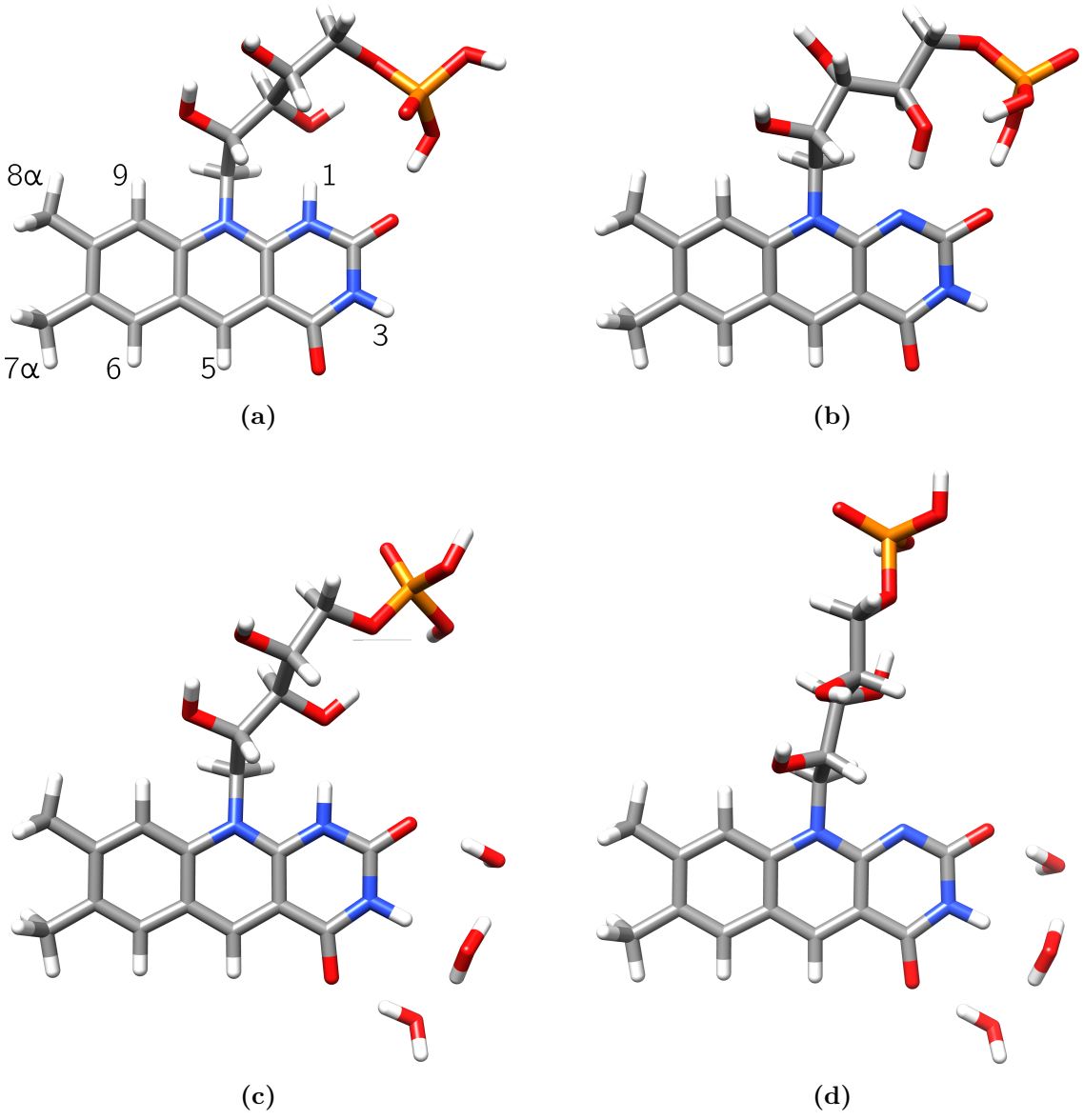

Figure S3 Optimized structures of 5-deazaFMN radicals used for the calculation of isotropic hyperfine coupling constants and isotropic g-values: (a) 5-deazaFMN(H1)$^{\bullet}$, (b) 5-deazaFMN$^{\bullet-}$, (c) 5-deazaFMN(H1)$^{\bullet}$ + 3 H_2O, (d) 5-deazaFMN$^{\bullet-}$ + 3 H_2O. The numbering of ^{1}H of the aromatic 5-deazaFMN moiety according to IUPAC nomenclature is given in (a).

Table S1 Calculated A_{iso} and isotropic g factors of anionic and neutral 5-deazaFMN radicals. Additionally, the two structures were modified by adding three H_2O molecules at specific positions. The structures are depicted in Fig. S3.A_{iso} are given in absolute and relative values. All relative values are normalized with respect to A_{iso} of H5.

	5-deazaFMN$^{\bullet-}$		5-deazaFMN(H1)$^{\bullet}$		5-deazaFMN$^{\bullet-}$ + 3 H_2O		5-deazaFMN(H1)$^{\bullet}$ + 3 H_2O	
g_{iso}	2.002799		2.002752		2.002822		2.002769	
	$A_{iso,abs}$ / MHz	$A_{iso,rel}$	$A_{iso,abs}$ / MHz	$A_{iso,rel}$	$A_{iso,abs}$ / MHz	$A_{iso,rel}$	$A_{iso,abs}$ / MHz	$A_{iso,rel}$
H5	−34.13	−1.00	−35.99	−1.00	−34.52	−1.00	−36.10	−1.00
H6	−11.55	−0.34	−11.23	−0.31	−11.38	−0.33	−11.30	−0.31
H7α	−4.18	−0.12	−4.06	−0.11	−4.14	−0.12	−4.23	−0.12
H8α	13.92	0.41	13.90	0.39	13.85	0.40	14.13	0.39
H9	2.92	0.09	3.30	0.09	3.14	0.09	3.54	0.10

5 Photo-CIDNP Experiments

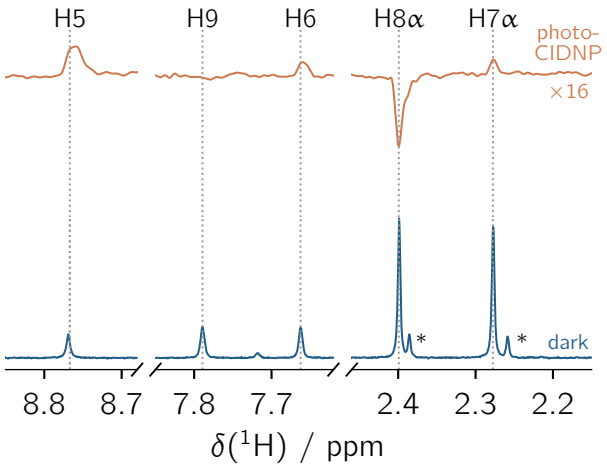

Figure S4 Thermally polarized (blue) and photo-CIDNP (orange) ^{1}H spectrum of 5-deazaFMN and L-tyrosine at pH 7.1. Only resonances of the aromatic moiety of 5-deazaFMN are shown. The sample was optically excited at 420 nm. The experiments were performed at 293 K with 128 and 48 scans, respectively. All resonances were referenced to the HDO signal at 4.7 ppm.

Table S2 Relative A_{iso} of 5-deazaFMN radicals obtained from photo-CIDNP experiments (see Fig. S5). The values are given with the pH value of the investigated sample. All values are normalized with respect to A_{iso} of H5.

pH	1.5	3.6	6.6	8.7	10.1
H5	−1.00	−1.00	−1.00	−1.00	−1.00
H6	−0.33	−0.38	−0.42	−0.26	−0.30
H7α	−0.08	−0.09	−0.09	−0.07	−0.08
H8α	0.35	0.40	0.41	0.41	0.39
H9	0.09	0.09	0.09	0.13	0.04

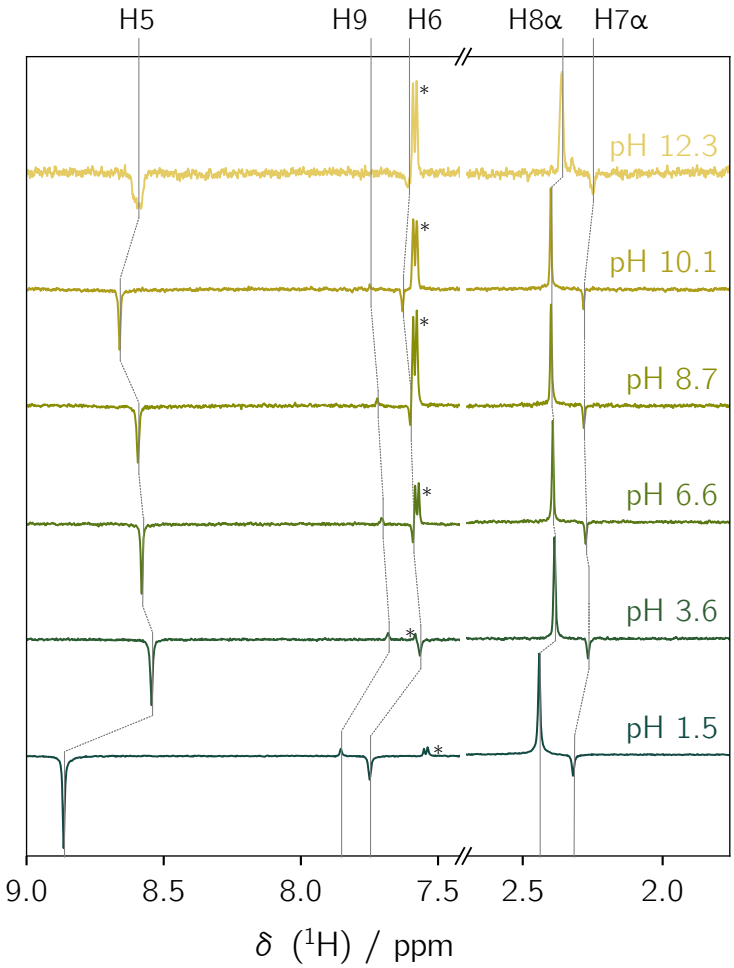

Figure S5 Photo-CIDNP experiments of 5-deazaFMN and L-tryptophan at pH values ranging from pH 1.5 to 12.3. The CIDNP signals are assigned to the respective proton of 5-deazaFMN. CIDNP signals of L-tryptophan are marked with asterisks. The samples were optically excited at 420 nm. The experiments were performed at 293 K with 1664, 512, 388, 1152, 512 and 384 Scans for pH 1.5 to pH 12.3 respectively.

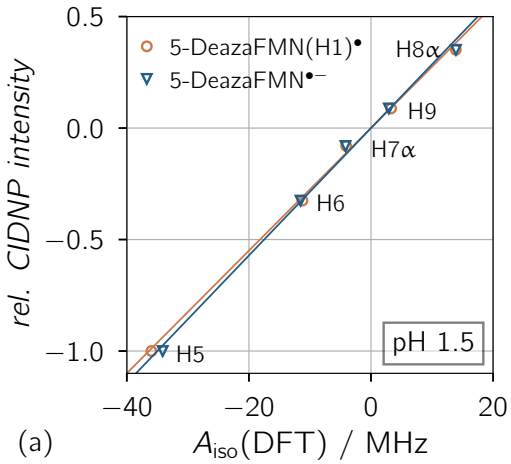
0.5
0.0
−0.5
−1.0
rel. CIDNP intensity
5-DeazaFMN(H1)•
5-DeazaFMN•−
H8α
H9
H7α
H6
H5
pH 1.5
−40
−20
0
20
(a)
Aiso(DFT) / MHz

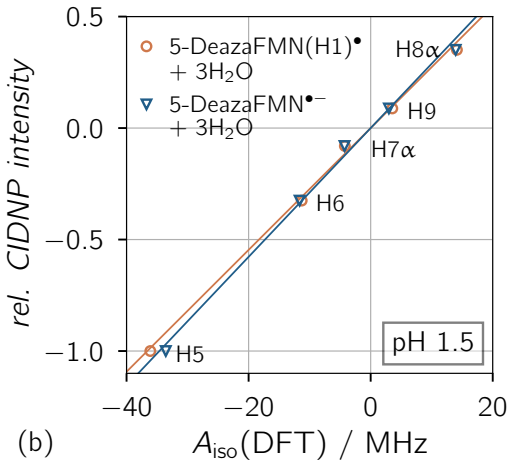
0.5
0.0
−0.5
−1.0
rel. CIDNP intensity
5-DeazaFMN(H1)•
+ 3H2O
5-DeazaFMN•−
+ 3H2O
H8α
H9
H7α
H6
H5
pH 1.5
−40
−20
0
20
(b)
Aiso(DFT) / MHz

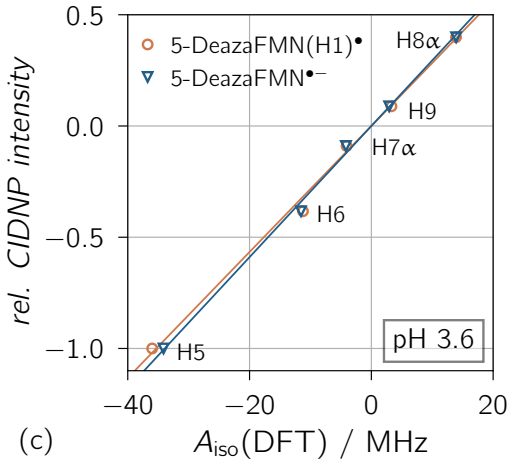
0.5
0.0
−0.5
−1.0
rel. CIDNP intensity
5-DeazaFMN(H1)•
5-DeazaFMN•−
H8α
H9
H7α
H6
H5
pH 3.6
−40
−20
0
20
(c)
Aiso(DFT) / MHz

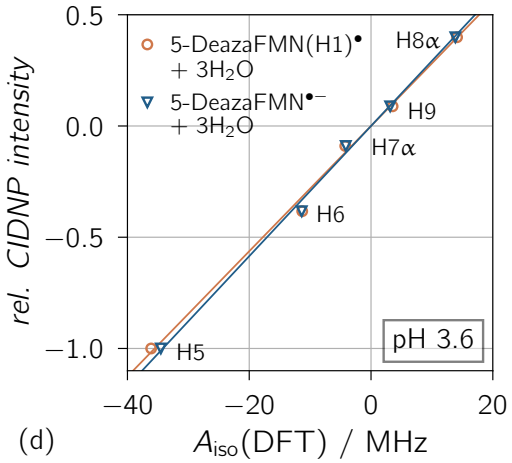
0.5
0.0
−0.5
−1.0
rel. CIDNP intensity
5-DeazaFMN(H1)•
+ 3H2O
5-DeazaFMN•−
+ 3H2O
H8α
H9
H7α
H6
H5
pH 3.6
−40
−20
0
20
(d)
Aiso(DFT) / MHz

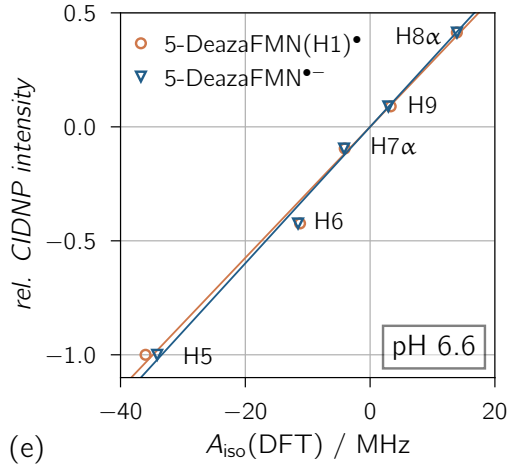
0.5
0.0
−0.5
−1.0
rel. CIDNP intensity
5-DeazaFMN(H1)•
5-DeazaFMN•−
H8α
H9
H7α
H6
H5
pH 6.6
−40
−20
0
20
(e)
Aiso(DFT) / MHz

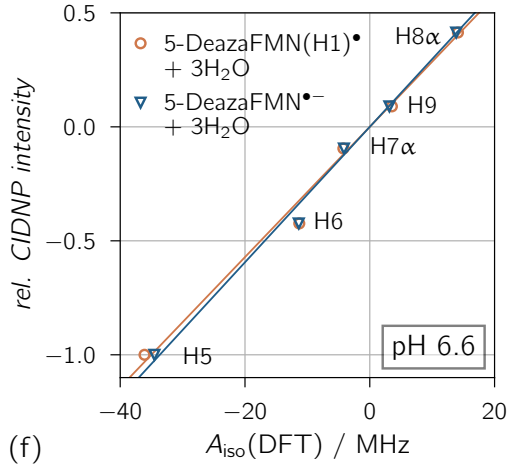
0.5
0.0
−0.5
−1.0
rel. CIDNP intensity
5-DeazaFMN(H1)•
+ 3H2O
5-DeazaFMN•−
+ 3H2O
H8α
H9
H7α
H6
H5
pH 6.6
−40
−20
0
20
(f)
Aiso(DFT) / MHz

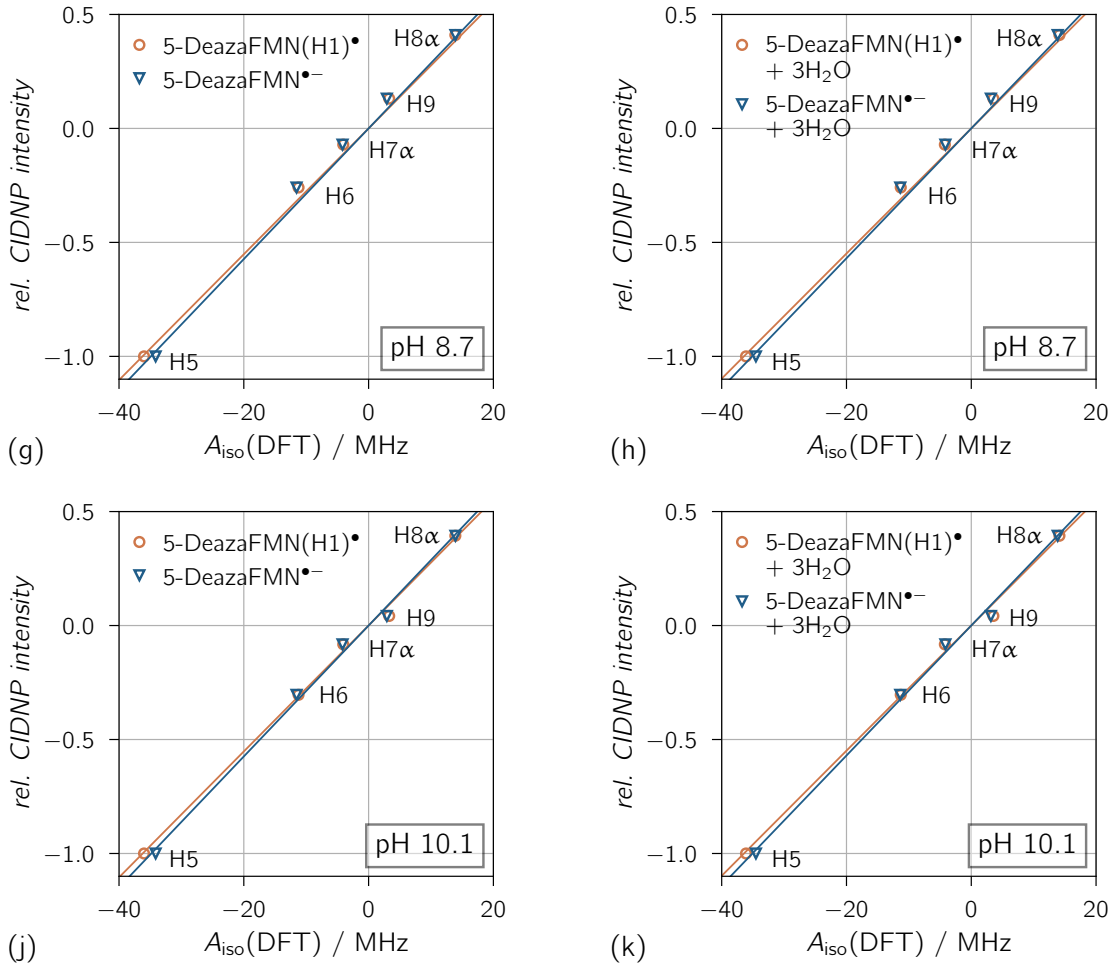

Figure S6 Linear regression fits of isotropic hyperfine coupling constants from DFT calculations and CIDNP experiments for the investigated 5-deazaFMN radical at (a) and (b): pH 1.5, (c) and (d): pH 3.6, (e) and (f): pH 6.6, (g) and (h): pH 8.7, (j) and (k): pH 10.1. CIDNP intensities were extracted from the experiments in Fig. S5. CIDNP intensities from the 5-deazaFMN radical at pH 12.3 were not evaluated due to poor signal-to-noise ratio. The fits were forced to go through the origin.

Table S3 Results of linear regression plots of isotropic hyperfine coupling constants from DFT calculations and CIDNP experiments. Given are the slope and the coefficient of determination for 5-deazaFMN$^{\bullet-}$ and 5-deazaFMN(H1)$^{\bullet}$.

	5-deazaFMN$^{\bullet-}$		5-deazaFMN(H1)$^{\bullet}$	
pH	slope / MHz^{-1}	R^2	slope / MHz^{-1}	R^2
1.5	0.0286	0.9960	0.0275	0.9980
3.6	0.0295	0.9973	0.0283	0.9954
6.6	0.0299	0.9937	0.0287	0.9899
8.7	0.0287	0.9959	0.0276	0.9989
10.1	0.0287	0.9960	0.0276	0.9968

Table S4 Results of linear regression plots of isotropic hyperfine coupling constants from DFT calculations and CIDNP experiments. Given are the slope and the coefficient of determination for 5-deazaFMN$^{\bullet-}$ + 3 H_2O and 5-deazaFMN(H1)$^{\bullet}$ + 3 H_2O.

	5-deazaFMN$^{\bullet-}$ + 3 H_2O		5-deazaFMN(H1)$^{\bullet}$ + 3 H_2O	
pH	slope / MHz^{-1}	R^2	slope / MHz^{-1}	R^2
1.5	0.0284	0.9968	0.0273	0.9975
3.6	0.0293	0.9968	0.0281	0.9953
6.6	0.0297	0.9927	0.0286	0.9900
8.7	0.0285	0.9971	0.0274	0.9986
10.1	0.0285	0.9961	0.0274	0.9960

6 Mulliken Spin Populations of FMN and 5-DeazaFMN Radicals

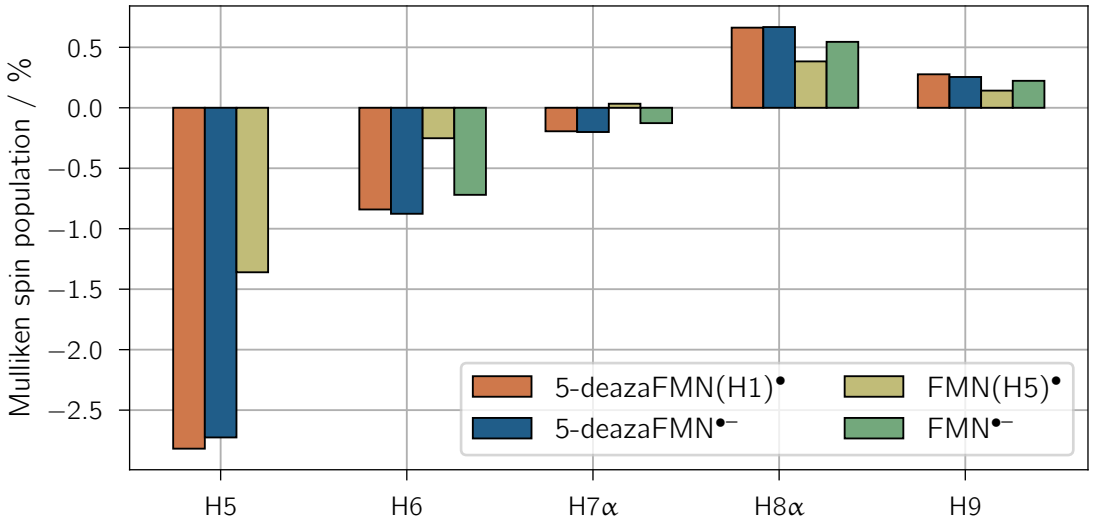

Figure S7 Comparison of ^{1}H Mulliken spin populations of 5-deazaFMN(H1)$^{\bullet}$ and 5-deazaFMN$^{\bullet-}$ as well as FMN(H5)$^{\bullet}$ and FMN$^{\bullet-}$.

Table S5 Mulliken spin populations in % of ^{1}H nuclei of FMN and 5-deazaFMN radicals in different protonation states. The values for ^{1}H nuclei of the isoalloxazine moiety are given.

Proton	5-deazaFMN(H1)$^{\bullet}$	5-deazaFMN$^{\bullet-}$	FMN(H5)$^{\bullet}$	FMN$^{\bullet-}$
H5	−2.8187	−2.7259	−1.3602	0.0000
H6	−0.8409	−0.8764	−0.2518	−0.7198
H7α	−0.1943	−0.2004	0.0335	−0.1269
H8α	0.6626	0.6677	0.3836	0.5452
H9	0.2769	0.2548	0.1420	0.2230

References

[1] D. E. O'Brien, L. T. Weinstock, and C. C. Cheng. Synthesis of 10-deazariboflavin and related 2,4-dioxopyrimido[4,5-*b*]quinolines (1a). *J. Heterocyclic Chem.* 7 (1970), pp. 99–105.

[2] N. Pompe, J. Chen, B. Illarionov, S. Panter, M. Fischer, A. Bacher, and S. Weber. Methyl groups matter: Photo-CIDNP characterizations of the semiquinone radicals of FMN and demethylated FMN analogs. *J. Chem. Phys.* 151, Art. No. 235103 (2019).

[3] M. Goez, K. H. Mok, and P. J. Hore. Photo-CIDNP experiments with an optimized presaturation pulse train, gated continuous illumination, and a background-nulling pulse grid. *J. Magn. Reson.* 177 (2005), pp. 236–246.

[4] F. Neese. The ORCA program system. *Wiley Interdiscip. Rev. Comput. Mol. Sci.* 2 (2012), pp. 73–78.

[5] F. Neese. Software update: The ORCA program system-Version 5.0. *Wiley Interdiscip. Rev. Comput. Mol. Sci.* 12, Art. No. e1606 (2022).

[6] P. J. Stephens, F. J. Devlins, C. F. Chabalowski, and M. J. Frisch. *Ab initio* calculation of vibrational absorption and circular dichroism spectra using density functional force fields. *J. Chem. Phys.* 98 (1994), pp. 11623–11627.

[7] A. Schäfer, C. Huber, and R. Ahlrichs. Fully optimized contracted Gaussian basis sets of triple zeta valence quality for atoms Li to Kr. *J. Chem. Phys.* 100 (1994), pp. 5829–5835.

[8] W. Kutzelnigg, U. Fleischer, and M. Schindler. "Deuterium and shift calculation". In: *NMR Basic Principles and Progress*. Ed. by U. Fleischer, W. Kutzelnigg, H.-H. Limbach, G. J. Martin, M. L. Martin, and M. Schindler. Berlin and Heidelberg: Springer, 1990, pp. 165–262.

[9] V. Barone and M. Cossi. Quantum calculation of molecular energies and energy gradients in solution by a conductor solvent model. *J. Phys. Chem. A* 102 (1998), pp. 1995–2001.

[10] J. Jeener, B. H. Meier, P. Bachmann, and R. R. Ernst. Investigation of exchange processes by two-dimensional NMR spectroscopy. *J. Chem. Phys.* 71 (1979), p. 4546.

[11] T. L. Hwang and A. J. Shaka. Water suppression that works. Excitation sculpting using arbitrary wave-forms and pulsed-field gradients. *J. Magn. Reson. A* 112 (1995), pp. 275–279.

[12] R. Wagner and S. Berger. Gradient-selected NOESY-A fourfold reduction of the measurment time for the NOESY experiment. *J. Magn. Reson. A* 123 (1996), pp. 119–121.